Trimers of the fibronectin cell adhesion domain localize to actin filament bundles and undergo rearward translocation

Françoise Coussen*, Daniel Choquet*, Michael P. Sheetz‡ and Harold P. Erickson‡,§

Department of Cell Biology, Box 3709, Duke University Medical Center, Durham, NC 27710, USA
*Present address UMR CNRS 5091, Université de Bordeaux 2, Institut François Magendie, 33077 Bordeaux, France
‡Present address: Department of Biological Sciences, Columbia University, New York, NY 10027, USA
§Author for correspondence (e-mail: h.erickson@cellbio.duke.edu)

Accepted 8 April 2002
Journal of Cell Science 115, 2581-2590 (2002) © The Company of Biologists Ltd

Summary

Previous studies have shown that small beads coated with FN7-10, a four-domain cell adhesion fragment of fibronectin, bind to cell surfaces and translocate rearward. Here we investigate whether soluble constructs containing two to five FN7-10 units might be sufficient for activity. We have produced a monomer, three forms of dimers, a trimer and a pentamer of FN7-10, on the end of spacer arms. These oligomers could bind small clusters of up to five integrins. Fluorescence microscopy showed that the trimer and pentamer bound strongly to the cell surface, and within 5 minutes were prominently localized to actin fiber bundles. Monomers and dimers showed only diffuse localization. Beads coated with a low concentration (probably one complex per bead) of trimer or pentamer showed prolonged binding and rearward translocation, presumably with the translocating actin cytskeleton. Beads containing monomer or dimer showed only brief binding and diffusive movements. We conclude that clusters of three integrin-binding ligands are necessary and sufficient for coupling to and translocating with the actin cytoskeleton.

Key words: Fibronectin, Cell adhesion, Signalling, Multivalent, Dimerization, Oligomer

Introduction

Integrins are transmembrane receptors that mediate cell adhesion by forming links between the extracellular matrix and cytoskeleton. These links are used in cell motility as the actin cytoskeleton generates force pulling the integrin and attached matrix molecules towards the cell center. On the ventral surface this rearward movement of the cytoskeleton contributes to forward motion of the cell relative to the substrate. Similar rearward translocation on the dorsal surface can be demonstrated by attaching beads to integrins. The movement of beads on the dorsal surface has been exploited to follow the pathway, velocity and forces developed by the cytoskeleton.

Two types of movement have been observed when beads are attached to integrins on the dorsal surface. Random diffusion is the initial and sometimes only movement, and is thought to indicate lack of attachment of the integrins to the cytoskeleton. When the bead-bound integrins attach to the cytoskeleton they stop diffusive movements and begin a rearward translocation at a constant velocity, typically 1-2 μm/minute (Schmidt et al., 1993). Two factors are important for attachment to the cytoskeleton and rearward translocation – clustering of the integrins and occupancy of the integrin by its matrix ligand. Felsenfeld et al. found that large (1 μm) latex beads coated with a non-interfering antibody against β1 integrin demonstrated rearward translocation, while small (40 nm) gold beads coated with the antibody showed only diffusive movements (Felsenfeld et al., 1996). When the concentration of antibody was reduced, even the large beads showed only diffusive movement, suggesting that integrin clustering was essential for cytoskeletal attachment. The study went on to show that small gold beads coated with FN7-10, a four-domain segment containing the central cell adhesion domain of fibronectin (FN), showed rearward translocation, implying that cytoskeletal attachment was significantly enhanced when the integrin was occupied by its FN ligand. Clustering was still essential, since beads coated with a low concentration of FN, probably one active molecule per bead, bound transiently to the cell but did not attach to the cytoskeleton or translocate.

Translocating beads coated with FN7-10 at first form a relatively weak attachment to the cytoskeleton, and they can be pulled off by a modest force using a laser trap (Choquet et al., 1997). However, when beads were subjected to a sustained force for 10 seconds or more, the cell increased the strength of the bond. The cell thus seems to be able to recruit additional cytoskeleton to attach a bead, allowing it to overcome an applied force and continue rearward translocation. This recruitment of cytoskeleton may be related to the findings that when FN-coated beads were placed in contact with a cell they induced formation of an actin cytoskeleton immediately beneath the point of bead binding (Miyamoto et al., 1995a; Miyamoto et al., 1995b). The formation of actin cytoskeleton upon bead contact, and the strengthening of attachment required both ligand binding and integrin clustering.

How many integrins are required to form a cluster that will attach to the cytoskeleton? To address this question we have made soluble oligomeric constructs with one, two, three and

five copies of the cell adhesion domain of FN, with the idea that these would form small clusters of two to five integrins. We found that clusters as small as three integrins rapidly bound to and decorated a set of actin fiber bundles, and mediated translocation when bound in single copies to small beads.

Materials and Methods

Construction of expression proteins

All expression proteins were produced with the expression vector pET11 [(Studier et al., 1990) Novagen], and are based on the expression protein FN7-10, previously described (Aukhil et al., 1993; Leahy et al., 1996). The protein constructs are shown in Fig. 1A. FN7-10 was used as a monomer control in some experiments, but we also constructed an FN-TN monomer, which contained the same TN spacer arm as the multimers (see below).

FN7-10 tandem dimer is a single polypeptide comprising two FN7-10 sequences separated by a GSGSHM linker. The second copy was amplified by PCR using pET-FN7-10 as a template, a forward primer inside the pET11b expression vector, and a reverse primer (5′-ATCATATGGGATCCCGAGCCTGTTCGGTAATTAATGGAAAT-3′). The reverse primer codes for ISINYRTGSGSHM, comprising the last seven amino acids of FN10, and a GSGSHM spacer (the final HM corresponds to the *Nde*I site added at the 3′ end). The PCR product was subcloned into the TA vector (Stratagene) and sequenced. The insert, containing *Nde*I at both the 5′ and 3′ ends, was cut out and inserted into the single *Nde*I site of pET-FN7-10. A clone with the correct orientation was selected.

FN-TN trimer was constructed to have FN7-10 at the N-terminus, followed by a spacer arm TN3-8 [comprising FN-III domains 3-8 from tenascin (Aukhil et al., 1993)] followed by the C-terminal trimer-forming sequence of chicken CMP (residues 451-492 EEDPCE...ENKII*) [for analysis of trimer assembly from the corresponding segment of human CMP, see Beck et al. (Beck et al., 1996)]. The pentamer was similar except that the oligomerization domain was the pentamer-forming sequence of human COMP [residues 27-83 GDLAPQ...GLSV* (Efimov et al., 1996; Malashkevich et al., 1996; Tomschy et al., 1996)]. Domains were amplified with a 5′ oligonucleotide containing an *Spe*I site (5′-TTCCTCACTAGTGAAGAAGATCCGTGCGAA-3′ for CMP; 5′-TTCCTCACTAGTGGAGACCTAGCCCCACAG-3′ for COMP) and a 3′ oligonucleotide containing a stop and *Bam*HI site (5′-GGATCCGAATTCCTAGATGATTTTGTTTTC-3′ for CMP; 5′-TCTCTCGGATCCGAATTCCTACACGCTCAGACC-3′ for COMP), subcloned in the TA vector and sequenced. Inserts were cut out and subcloned in a Litmus-29 vector containing *Spe*I and *Bam*HI sites in the polycloning site. DNA corresponding to FN-III domains 3-8 of tenascin was amplified with a 5′ oligonucleotide containing an *Nde*I site and a 3′ oligonucleotide containing an *Spe*I site, and subcloned into the Litmus-29 vector in front of CMP or COMP cDNA. Inserts were cut out of Litmus-29 with *Nde*I and *Bam*HI and ligated into pET 11b vector cut by *Nde*I and *Bam*HI. Control proteins TN3-8CMP and TN3-8COMP (lacking the FN7-10 segment) were expressed from these vectors. Finally, FN7-10 DNA with *Nde*I at each end was ligated into the *Nde*I site of these vectors, and clones with the correct orientation were selected.

FN-TN dimer utilized the 28 amino acid model coiled-coil segment (EIEALKAEIEALKAEIEALKAEIEALKA) from the K6 peptide (Tripet et al., 1997), which was designed to form a stable two-stranded coiled coil. This segment was constructed by a set of PCR reactions. The first PCR used as template an oligonucleotide corresponding to the central segment of the K6 peptide (5′-GAAGCATTAAAG-GCTGAAATTGAGGCTCTAAAGGCTGAAATC-3′) and primers overlapping this and extending it in both directions: forward (5′-GCACTCAAGGCTGAAATCGAAGCATTAAAGGCTGAA-3′) and reverse (5′-TAGAGCTTCGATTTCAGCCTTTAGAGC-3′). This first PCR product was then amplified with a set of two primers containing the 5′ (5′-ACTAGTGAGATAGAAGCACTCAAGGCTGAAATC-3′) and 3′ (5′-GGATCCCTATGCCTTTAGAGCTTCGATTTCAGC-3′) ends with the corresponding *Spe*I and *Bam*HI restriction sites. The final PCR product was subcloned in the TA vector and sequenced, and then inserted into the trimer vector, replacing the *Spe*I-*Bam*HI segment containing CMP. Finally, the FN-TN monomer was constructed by subcloning the FN7-10 segment into a pET11b containing TN fn3-8, using appropriate restriction fragments.

FN-MukBcoil is a construct that places an FN7-10 at each end of a long antiparallel coiled coil, with a flexible hinge in the middle. Construction and purification of the dimeric FN-MukBcoil has been described previously (Melby et al., 1998).

Expression in *E. coli* and purification of the proteins

Plasmids were transformed into *E. coli* BL21(DE3). Protein expression was induced at A600=0.7 by adding 0.4 mM IPTG for 3 hours. Bacteria were extracted with lysozyme and 0.1% Triton X-100, followed by two cycles of freeze-thaw. Following centrifugation, all expressed proteins were in the bacterial supernatant. Proteins were precipitated with ammonium sulfate, using the following percentage saturation: FN7-10 monomer, 40%; FN-FN tandem dimer, 40%; FN-TN monomer, 40%; FN-TN dimer 35%; FN-TN trimer 30%; and FN-TN pentamer, 25%. The ammonium sulfate pellets were resuspended in column buffer (0.02 M Tris, pH 8, containing 0.1 M NaCl if it is to be run over a Sephacryl column). FN7-10 monomer and FN-FN tandem dimer proteins were run directly over a mono Q column (Amersham-Pharmacia; or resource Q, which seems equivalent). All proteins containing TN spacer arm were run over a Sephacryl 100 or Sephacryl 500 column (Amersham-Pharmacia) following ammonium sulfate precipitation, and the peak fractions were applied to the mono Q column. All the proteins eluted from the mono Q between 0.2 and 0.3 M NaCl. With the trimer and pentamer we had the highest yield (5-10 mg per liter of bacteria) when the purification was completed in 1 day; storing or freezing samples before the mono Q step resulted in precipitation and loss of protein, as did diluting the salt below 0.1 M. We discovered that the FN trimer and pentamer precipitated in low salt, so we introduced a final purification step dialyzing them into 20 mM Tris with no salt, collecting the precipitate by centrifugation and resuspending it in Tris containing 0.2 M NaCl. On non-reducing gels, the trimer and pentamer showed a mixture of oligomers (up to trimer and pentamer, respectfully), suggesting only partial formation of disulfide bonds. Other studies have shown that oligomerization is driven primarily by the formation of the coiled coil, and that disulfide bond formation is not essential (Beck et al., 1996; Efimov et al., 1996).

Electron microscopy

HPLC fractions containing the proteins of interest were further purified by gradient sedimentation on a 15-40% glycerol gradient in 0.2 M ammonium bicarbonate. Peak fractions were rotary shadowed and examined by electron microscopy (Fowler and Erickson, 1979).

Cell surface localization

Experiments were performed on NIH 3T3 mouse fibroblasts transfected with a cDNA encoding the chick integrin β1 subunit as described (Choquet et al., 1997). Cells were cultivated in DMEM supplemented with 10% fetal calf serum, 1% penicillin/streptomycin/glutamine, kept at 37°C in a 5% CO_2 incubator and passaged every 3-4 days. The day before the experiment, cells were plated at 10^4 cells/ml on laminin-coated, silanized glass coverslips in the same culture medium without phenol red and with 10 mM Hepes, pH 7.2 (Schmidt et al., 1993).

Proteins were dialyzed in phosphate buffered saline (PBS: 8 g/l NaCl, 0.2 g/l KCl, 0.2 g/l KH_2PO_4, 1.15 g/l $NaHPO_4$, pH 7.2)

overnight and biotinylated as described (Choquet et al., 1997). An important point was to centrifuge the protein (13,000 ***g*** for 15 minutes) after biotinylation and prior to the experiment. Without the centrifugation a weak staining of streaks was also seen with monomeric and tandem-dimer FN7-10 preparations, probably due to a small quantity of protein aggregates produced during the biotinylation. Unless otherwise indicated, cells were incubated at 37°C with media containing 700 μl of 3 μM purified proteins. Molarity refers to the concentration of FN7-10 subunits, so 3 μM is 120 μg/ml for FN7-10 monomer and tandem dimer, and 300 μg/ml for FN-TN dimer, trimer and pentamer. After 30 seconds to 10 minutes, cells were directly fixed by addition of 4 ml of 3% paraformaldehyde at 37°C for 10 minutes. Coverslips were rinsed with PBS containing 0.1 M glycine and 2% bovine serum albumin (BSA) for 10 minutes and with PBS-BSA for 5 minutes. They were then incubated for 20 minutes with 5 μg/ml fluorescent avidin neutralite (Molecular Probes, Eugene, OR) in PBS/BSA buffer, and were washed with PBS buffer before mounting.

Under some culture conditions the cells assembled a FN matrix. When FN fibrils were present they decorated strongly with all of the vectors that contained TN3-8, regardless of the presence of FN7-10. TN3-8 is known to bind FN fibrils (Chung et al., 1995), so this decoration was not surprising. We found that it could be inhibited by adding an excess of TN3-8 pentamer to the labeling mixture, so this was included in most of the decoration experiments.

For phalloidin staining of actin, cells were permeabilised with 0.3% Triton X-100 for 5 minutes, rinsed in PBS/BSA buffer and incubated simultaneously with Alexa 568-phalloidin (Molecular Probes) and fluorescent avidin. Phalloidin concentration was adjusted so there was no bleed-through on the green channel. Staining with anti integrin-α5 antibody (monoclonal, hamster anti-mouse CD49, Pharmingen) was carried out after fixation for 30 minutes at room temperature. Secondary antibody (Texas Red goat anti-Armenian-hamster antibody) was incubated together with the FITC-avidin, to provide double labeling of bound FN oligomers and α5 integrin. In both cases the incomplete overlap shows that the co-localization is not due to bleed-through of the fluorescent labels.

Video-microscopy of bead binding

Carboxylated latex beads (Polyscience, Warrington, PA) were coated with biotinylated BSA using a carbodiimide linkage (Kuo and Sheetz, 1993) and stored at 4°C. Prior to the experiment, beads were incubated overnight at 4°C with 2 mg/ml avidin neutralite (Molecular Probes). After PBS-BSA washes, beads (2% solution) were incubated for 1 hour at room temperature with the various biotinylated FN7-10 proteins (30-100 ng/ml), and then washed with PBS-BSA. Coated beads were made freshly every day.

Before the experiments, cells were mounted in a chamber consisting of two coverslips separated by 1 mm spacers. The cells were mounted with 200 μl centrifuged culture medium supplemented with 1 μl of a 2% solution of beads. Cells were visualized with a 1.3 NA 100 X plan-neofluar objective on an Axiovert 100 TV inverted microscope, equipped with Nomarski optics. The chamber and objective were maintained at 37°C by flowing heat regulated air.

The experimental setup for optical tweezers was essentially as described (Kuo and Sheetz, 1993). An Innova 70 Argon laser pumped an 890 Titanium-Sapphire laser (Coherent, Bowie, MD) set at 800 nm and 100-150 mW of output power. The expanded beam was used to form an optical trap. Video frames were digitized and a single particle tracking program used to detect bead position with a sensitivity of 5-10 nm for 1 μm beads (Gelles et al., 1988; Schmidt et al., 1993). The 2D diffusion coefficient D and bead velocity V were computed by fitting the function $f(t)=4Dt+bt^2$ to the curve of mean squared displacement versus time, f(t) (Qian et al., 1991). If b was negative or null, the track was said to be purely diffusive movement, otherwise, the velocity of directed displacement was taken as the square root of b. We have performed Student's *t*-tests on the different sets of data.

Results

Protein expression, purification and characterization

The schematic diagram of the constructs is shown in Fig. 1A, and a scale model of the FN-TN trimer protein in Fig. 1B. FN7-10 monomer and FN-FN tandem dimer consist of a single or double copy of the cell adhesion segment of FN. FN-MukB dimer uses the antiparallel coiled coils of the bacterial protein MukB, which comprises two 50 nm long arms connected by a flexible hinge (Melby et al., 1998). One FN7-10 segment is placed at each end, as previously described (Melby et al., 1998). All the other constructs place the FN7-10 on a TN3-8 spacer arm, which is a 21 nm long, 6-domain segment from tenascin (FN-III domains 3-8). These are assembled into dimers, trimers or pentamers by adding a short coiled-coil segment at the C-terminus. The dimer uses the artificial K6 peptide, designed to form a very stable two-stranded coiled coil (Tripet et al., 1997). The trimer uses a short segment from cartilage matrix protein (CMP) that forms a three-stranded coiled-coil (Beck et al., 1996), and the pentamer a segment from cartilage oligomeric matrix protein (COMP), which forms a five-stranded coiled-coil (Efimov et al., 1996; Malashkevich et al., 1996; Tomschy et al., 1996). In addition to the constructs containing FN7-10, we made control trimers and pentamers containing only the TN3-8 spacer arms. EM of the purified proteins (Fig. 2) largely confirmed the expected structures, with some interesting variations.

FN7-10 monomer is the cell adhesion domain of FN, whose structure was determined by X-ray crystallography (Leahy et al., 1996). EM shows short rods close to the expected 14 nm length (Fig. 2). FN-FN tandem dimer consists of two of these segments connected by a short flexible linker. EM shows these to be about twice the length of FN7-10 monomer, sometimes bent into a V.

FN-TN monomer should have a length of 35 nm (3.5 nm per domain), but electron microscopy revealed a bimodal distribution, with peak lengths of 32 nm and 60-70 nm. Fig. 2 shows examples of the short and longer molecules in this fraction. The short molecules correspond to true monomers, while the longer molecules appear to be end-to-end dimers. A number of strands with a length of 90-100 nm, and a few longer ones, were found, which are apparently trimers and larger strands. The presence of these larger strands suggests a head to tail association of the C-terminal interface of TN8 with the N-terminal interface of FN7. The tendency of FN-TN monomer to dimerize was also indicated in sedimentation equilibrium, and by the fact that it sedimented in glycerol gradients at 4.6S, exactly the same as FN-TN dimer (data not shown). About 60% of the molecules in a typical FN-TN monomer preparation appeared to be dimers and 30% were monomers. Therefore this FN-TN monomer is not a good control as a monomer, but rather provides an additional construct that is mostly dimeric.

The FN-TN dimer based on the coiled coil also showed two peaks of lengths, with a major peak at 65 nm and a smaller peak at 33 nm. The monomers in this fraction could result from incomplete association of the coiled coils or from proteolysis. About 60% of the molecules in the dimer preparation appeared

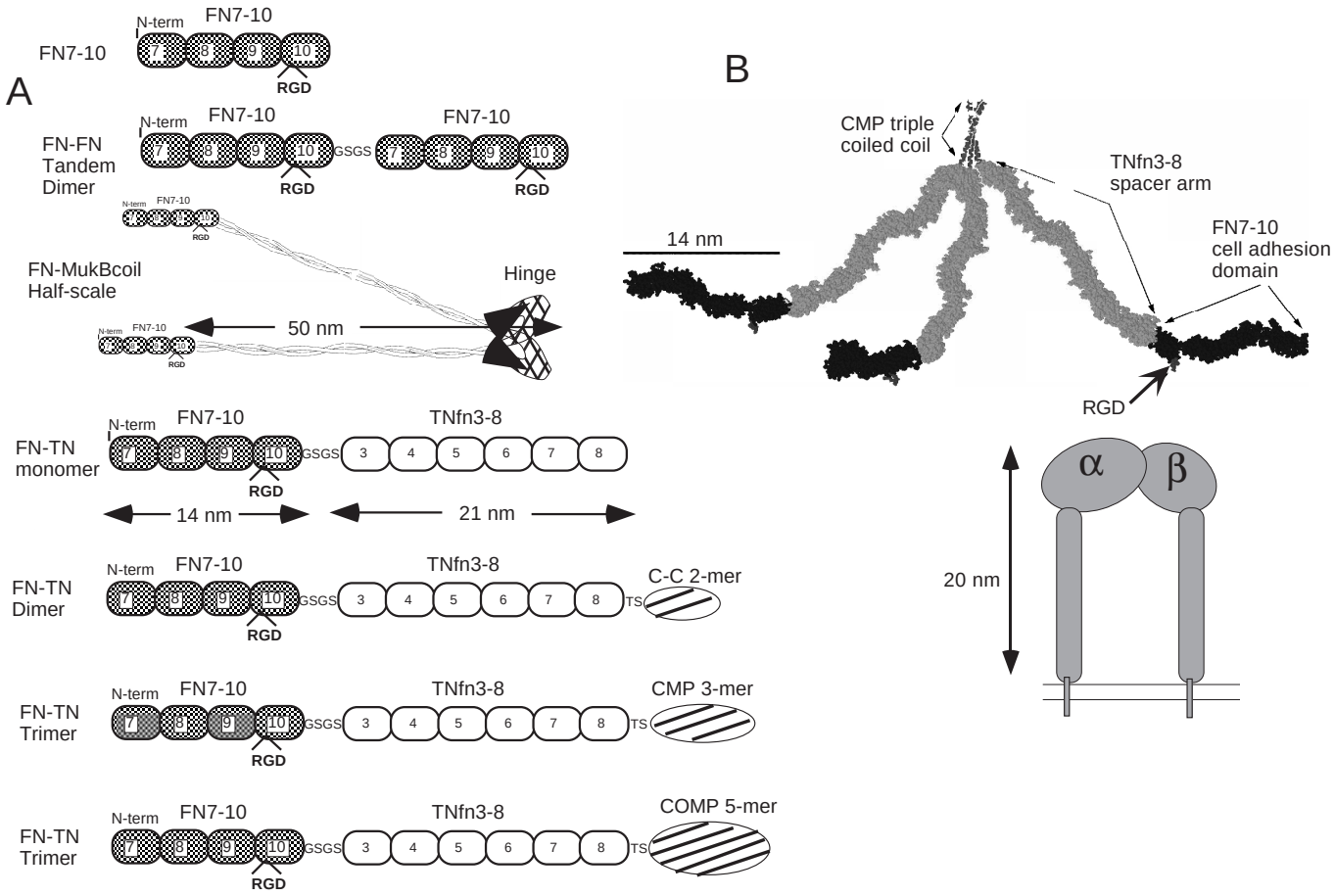

Fig. 1. (A) Constructs for multimeric FN7-10 (see Materials and Methods for details). (B) A scale model of the FN7-10 trimer, constructed from the coordinates of FN7-10 (Leahy et al., 1996) (these were also used to model the six FN-III domains in TNfn3-8) with the program RasMol (Sayle and Milner-White, 1995). The FN3 domains are shown as a spacefilling atomic model, and the α-helices of CMP are indicated schematically in a ribbon format. For comparison an integrin molecule is drawn to scale (Carrell et al., 1985; Nermut et al., 1988).

to be dimers (65±10 nm). Almost all of the dimers showed the two arms projecting in opposite directions in a straight line, with rarely a hint of a bend at the middle. This suggests that the C-terminal interfaces of TNfn8 have a tendency to associate with each other.

EM of the trimer and pentamer showed multi-arm oligomers (Fig. 2). The control proteins with the tenascin spacer arms (lacking the FN7-10 segment) gave the most reproducible structures, with most of the molecules having the expected 3 or 5 arms. The FN-TN constructs frequently appeared to be missing an arm. We estimate that more than half of the trimers and pentamers showed the full complement of arms, and only a small fraction were missing more than one arm, as observed by EM. Because the control TN trimers and pentamers showed mostly the correct number of arms, we believe the apparent missing arms in the FN-TN constructs may be due to a weak association of the FN segments within the oligomer. If the missing arms are obscured by binding to each other, the fraction of intact trimers and pentamers is probably near 100%. Gel electrophoresis showed no evidence of proteolysis, consistent with this prediction.

Given that the FN-TN monomer tended to dimerize, it was important to establish that the other constructs did not associate into complexes larger than the trimer or pentamer. Glycerol gradient sedimentation gave sedimentation coefficients of 4.6S for both FN-TN monomer and dimer (consistent with the EM results that the monomer is actually a dimer), 5.8-5.2S for trimer and 7.7S for pentamer. We found that at higher protein concentrations both the trimer and pentamer tended to aggregate, especially in low salt. Gradient sedimentation and high speed centrifugation experiments performed in DMEM demonstrated significant aggregation of trimer at 2 mg/ml (20 μM subunits), but negligible aggregation at 1, 0.5 and 0.25 mg/ml. The experiments reported here were all done at a maximum concentration of 0.3 mg/ml, where we found no indication of aggregation.

One of the most important points of the geometry of the constructs is the spacing of bound integrins. The integrin should be centered between FN10 (with the RGD) and FN9 (the synergy domain), which is 24.5 nm from the hinge region of the FN-TN oligomers. The maximum separation of bound integrins will therefore be 49 nm, while an ‘average’ spacing of 35 nm will be obtained when the arms are at a 90 degree angle. For FN-MukBcoil the maximum spacing will be 113 nm. All of the constructs were designed to have flexible hinges, and can bring integrins into contact with each other. For reference, the width of an integrin head is 8-12 nm (Fig. 1B).

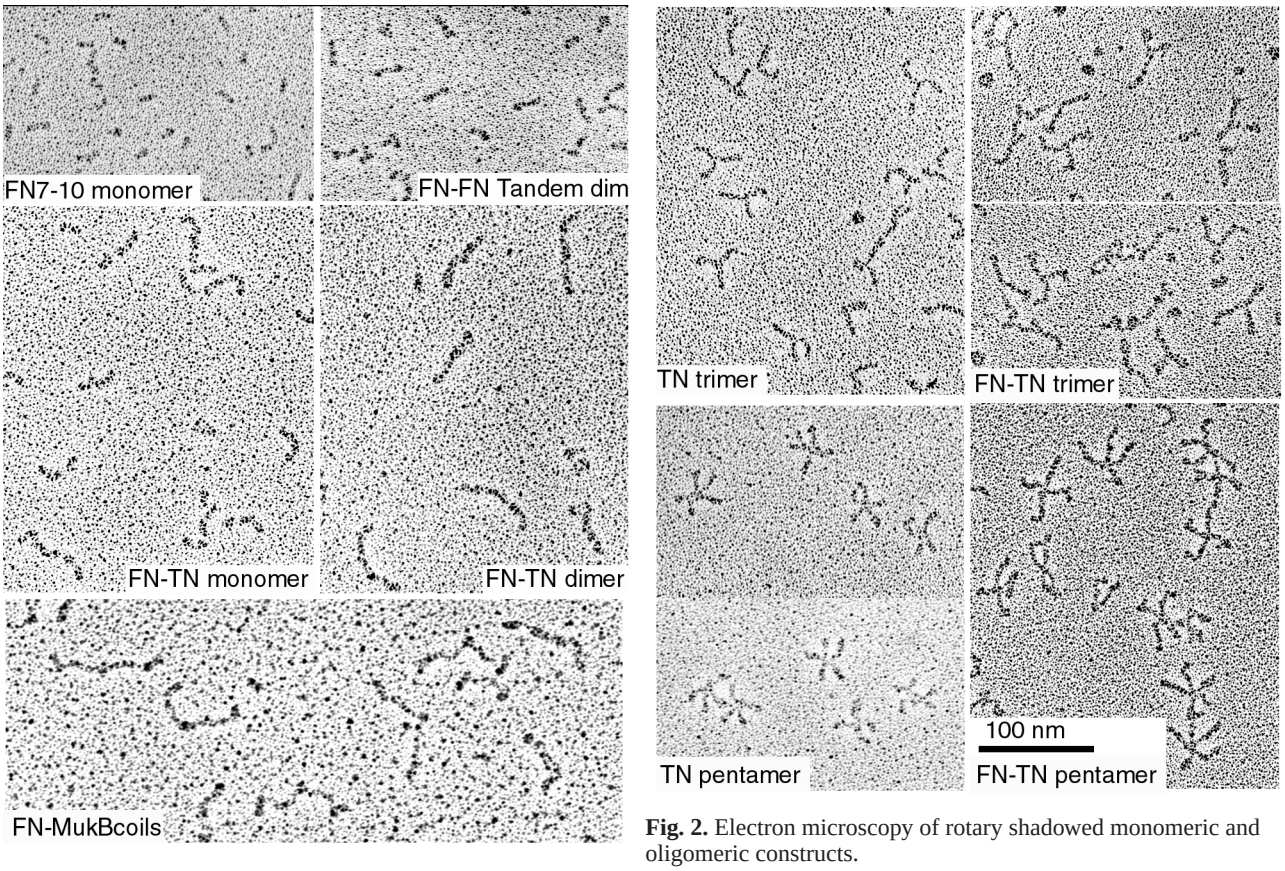

Fig. 2. Electron microscopy of rotary shadowed monomeric and oligomeric constructs.

Binding and distribution of FN7-10 on the surface of fibroblasts

Binding of FN7-10 constructs to motile, non-confluent fibroblasts was tested by adding the biotinylated proteins at 3 μM (the concentration of FN7-10 subunits) for 2.5 minutes (Fig. 3), followed by fixation and staining with FITC-avidin. FN7-10 monomer stained the cells weakly, showing some binding to the apical membrane and some dots on the lamellipodia. Increasing the concentration of FN7-10 monomer by tenfold increased the level of staining, but the pattern remained diffuse. FN-FN tandem dimer gave a diffuse staining pattern very much like that of the monomer, but the staining was sometimes more intense. The number and intensity of dots on the lamellipodia were the same with monomer and tandem dimer. The monomer and dimer panels showed some localization to streaks (Figs 4, 5) but these were always much weaker and fewer in number than with the trimer and pentamer.

The binding and distribution of the FN-TN trimer was strikingly different. Between 80 and 90% of the cells displayed streaks of intense staining running from the leading edge of the cell across the lamellipodia towards the center of the cell. The intensity of staining was very high compared with cells stained with monomer or tandem dimer. Confocal microscopy indicated that these streaks were on the top of the cells (not shown).

FN-TN pentamer gave a staining pattern similar to that of the trimer, but the streaks were even more intense. Many streaks ran all the way from the leading edge to the center of the cell. Even at 2.5 minutes of incubation with the pentamer, some cells started to retract their lamellipodia and round up. These cells often displayed hot spots of staining at the base of the lamellipodia, perhaps representing internalized protein (Fig. 3, right-hand images of tandem dimer and pentamer). In cells treated with FN7-10 pentamer almost all of the fiber bundles were visible by DIC. This may be because the lamellapodia were starting to contract and had less cytoplasm, but it is also possible that the fiber bundles had got thicker due to contraction or accumulation of extra actin.

We were surprised that the tandem dimer had no activity, since we expected receptor dimerization to be the principle of activation. We therefore constructed two new dimers: one had a TN spacer arm identical to that of the trimer and pentamer; and the other was based on the antiparallel coiled coil MukB, and had longer arms than the FN-TN dimer (Fig. 1). These new dimer constructs gave a weak and mostly diffuse staining pattern identical to that of the tandem dimer. In order to verify the specificity of the staining, we constructed a control trimeric protein containing the TN3-8 spacer arms, but lacking the FN7-10 domains. This construct gave negligible binding to cells (Fig. 3, bottom left). However, we should note that under some cell culture conditions the cells assembled FN matrix fibrils, and these fibrils stained strongly with all constructs containing the TN spacer arm, consistent with the known affinity of TN for FN fibrils (Chung et al., 1995). We have not discovered the conditions favoring or inhibiting FN matrix assembly.

Competition of FN7-10 monomer

We also tested the ability of FN7-10 monomer to compete for

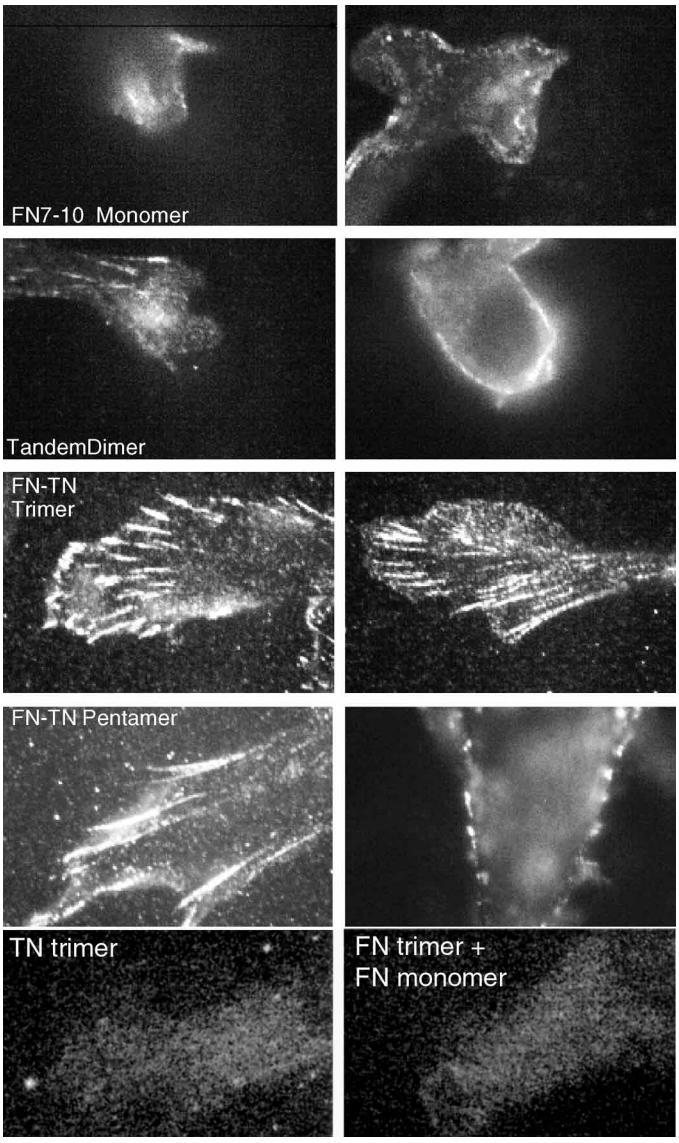

Fig. 3. Distribution of FN7-10 monomers and oligomers bound to fibroblasts. Soluble biotinylated proteins at 3 μM (subunit concentration) were added to fibroblasts grown overnight on a laminin substrate. After 2.5 minutes the cells were fixed and stained with fluorescent avidin to localize bound FN. Two examples are given for each protein. For the tandem dimer and pentamer, the focal plane of the right hand images was set above the substrate to optically section at the level of the cell body, illustrating the diffuse membrane staining for the tandem dimer and the punctate staining for the pentamer. For all other images the focus was on the upper surface of the lamellapodia. Control TN trimer (lacking the FN7-10 segment) does not bind the cell surface (bottom left). A competition experiment is shown in the bottom-right panel, where cells were treated with 3 μM biotinylated FN7-10 trimer in the presence of 30 μM unbiotinylated FN7-10 monomer. Binding of trimer is efficiently competed by excess monomer.

binding of the FN-TN trimer. When cells were treated with labeled FN-TN trimer at 3 μM, plus unlabeled FN7-10 monomer at 30 μM, the staining of the streaks was completely inhibited (Fig. 3, bottom-right).

The above experiments were done with subunit concentrations of 3 μM, but Fig. 4A shows that binding and labeling of streaks can be obtained at lower concentrations. FN-TN trimer gave very little labeling of streaks at 0.1 and 0.2 μM, but streaks were prominently labeled at 0.5 and 1.0 μM. We explored the competition by monomer using 0.5 μM FN-TN trimer. Fig. 4B shows that labeling of streaks is unaffected by up to 0.75 μM FN7-10 monomer, but is reduced somewhat at 2.25 μM, a 4.5-fold excess. Staining is greatly reduced at 3.0 μM or greater concentration of monomer, a sixfold excess. This is consistent with the results in Fig. 3, where a tenfold excess of monomer completely blocked staining by 3 μM trimer.

Time course of the binding for the different proteins

To study the behavior of the cells as they bind the proteins, we incubated them with 3 μM protein for 30 seconds to 10 minutes at 37°C. For the monomer, only weak staining was apparent at 30 seconds and 2.5 minutes. At 5 and 10 minutes some small spots were observed on the lamellipodia although they were weak. FN-FN tandem dimer gave almost the same pattern except for a higher staining at the tip of the leading edge and the appearance of a few weak streaks.

FN-TN trimer give the characteristic pattern of streaks for the whole time course of the experiment. At 30 seconds of incubation the intensity of staining was weak, but the pattern of streaks was already visible. At 2.5 minutes the staining of streaks was increased substantially in intensity, and was present on almost all cells. These streaks were stable and tended to be more intense after 10 minutes.

FN-TN pentamer gave a pattern of streaks very similar to the trimer, but the staining was even more intense. The streaks stained by pentamer were deeper than with the trimer, extending closer to the cell nucleus. In contrast to the trimer, where the cells and pattern of streaks remained static for 10 minutes, the pentamer caused cells to round up and aggregate the bound FN-TN at the base of the nucleus. This was already apparent for some cells at 5 minutes, and at 10 minutes almost 80% of the cells were rounded.

FN7-10 trimer localizes α5 β1 integrin to actin bundles

We confirmed the expectation that the FN-TN constructs are binding to integrins by colocalization. Fig. 5 shows that cells treated with FN-TN monomer or dimer had a diffuse distribution of α5-integrin. In cells treated with FN-TN trimer or pentamer the diffuse distribution of integrin remained, but some integrin was now associated into streaks. These streaks of integrin coincided with the streaks of FN-TN. The distribution of plasma FN (bottom two panels) was notably different. It generated streaks of α5 integrin and co-localized with them, but there were also substantial patches of FN located outside these streaks.

The pattern of streaks resembles that of actin fiber bundles, and indeed in many cells the fibers showed visible contrast with differential interference optics. To confirm the identity of these fibers, cells were stained simultaneously for bound FN-TN and with phalloidin to stain F-actin (Fig. 6). All the streaks of FN-TN trimer and pentamer were localized over F-actin fibers, but the actin was more extensive than the labeled streaks. Thus some actin fibers were not labeled at all, and

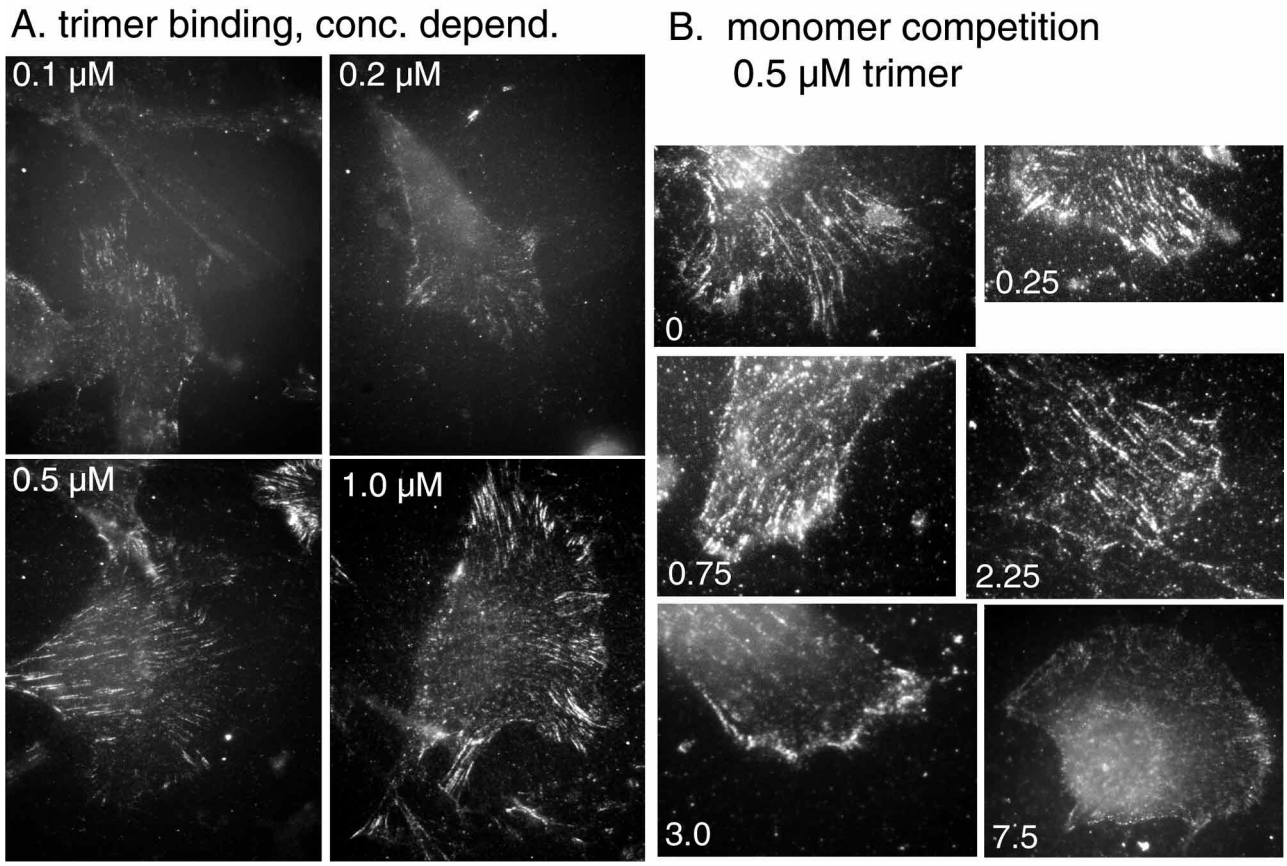

Fig. 4. (A) Binding of FN-TN trimer to fibroblasts at different concentrations. At 0.5 μM and above the trimer localizes to streaks on the cell surface. (B) Competition of trimer binding by FN7-10 monomer. The trimer was at 0.5 μM and FN7-10 monomer was varied. In both A and B 20 μM TN pentamer was included to compete and block binding to FN fibrils. Cells were incubated with the trimer or trimer plus monomer for 4 minutes, then fixed and stained with fluorescent avidin.

most were labeled only over a portion of their length. The occasional small streaks on cells labeled with FN-TN monomer or dimer were also localized over actin fibers. In cells labeled with plasma FN some of the FN localized over actin fibers, but there were some patches of FN elsewhere. The binding of whole FN dimers may involve receptors in addition to α5β1. The pattern of actin fibers appeared to be the same in cells treated with all the constructs (Fig. 6), and in untreated cells (not shown). This suggests that the FN-TN multimers are localizing to pre-existing actin fibers, rather than inducing their assembly.

Particle tracking of FN7-10-coated latex beads

To follow the movement of integrins on the cell surface we performed single particle tracking experiments with beads coated with the monomeric and multivalent FN. Our aim was to ensure that beads were bound to the cell through a single protein complex, in order to vary the aggregation level of the integrins solely by changing the valency of the protein. For that purpose, we coated the beads with a low protein concentration, so that on a given experiment only 20-25% of the beads displayed binding to the cell. We reasoned that a high fraction of beads would then be bound to cells through a single complex.

An optical laser trap was used to pick floating beads in the medium and put them in contact with the lamellipodia for a fixed time (4 seconds). The trap was then released and the behavior of the bead was followed by single particle tracking (Fig. 7).

Beads coated with FN7-10 or FN-TN monomer behaved identically, displaying very short binding to the cell surface (mean binding 1-2 seconds) and diffusive movements while bound. This means that the association of monomeric FN7-10

Table 1. Differential behavior of beads coated with FN7-10 multimers

	% Diffusive	% Immobile	% Rearward moving	*n*
Monomer	76	4	20	114
Dimer	43	35	22	102
Trimer	18	16	66	50
Pentamer	31	6	63	16

Beads were coated with the different constructs and their trajectories on cell lamellapodia were recorded and analyzed as described in Materials and Methods. Beads with a diffusion coefficient $>2\times10^{-10}$ cm^2/second were scored as diffusive. Beads with a diffusion coefficient $<2\times10^{-10}$ cm^2/second and no velocity were scored as immobile while those displaying directed movement were scored as rearward moving. For this tabulation, FN7-10 monomer and FN-TN monomer were pooled, as were FN-FN tandem dimer and FN-TN dimer.

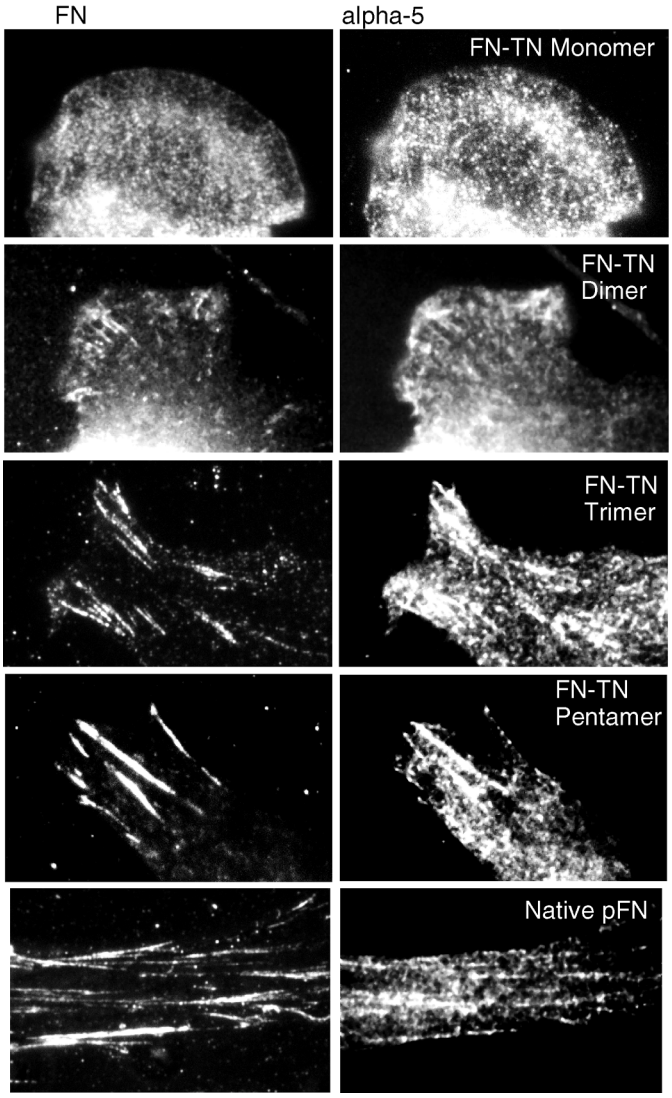

Fig. 5. Localization of α5-integrin induced by FN trimer and pentamer. Cells were treated for 5 minutes with different FN-TN constructs and then fixed and labeled simultaneously with avidin to localize the FN-TN construct, and with an antibody against α5-integrin. The monomer and dimer show mostly a diffuse pattern of both FN and integrin. The trimer and pentamer show the strong localization of FN into streaks, as already described. These streaks also stained for α5 integrin, although a substantial pool of diffuse integrin remained in each case. Some plasma FN (pFN) localized over the integrin streaks, but there were also prominent FN patches localized elsewhere.

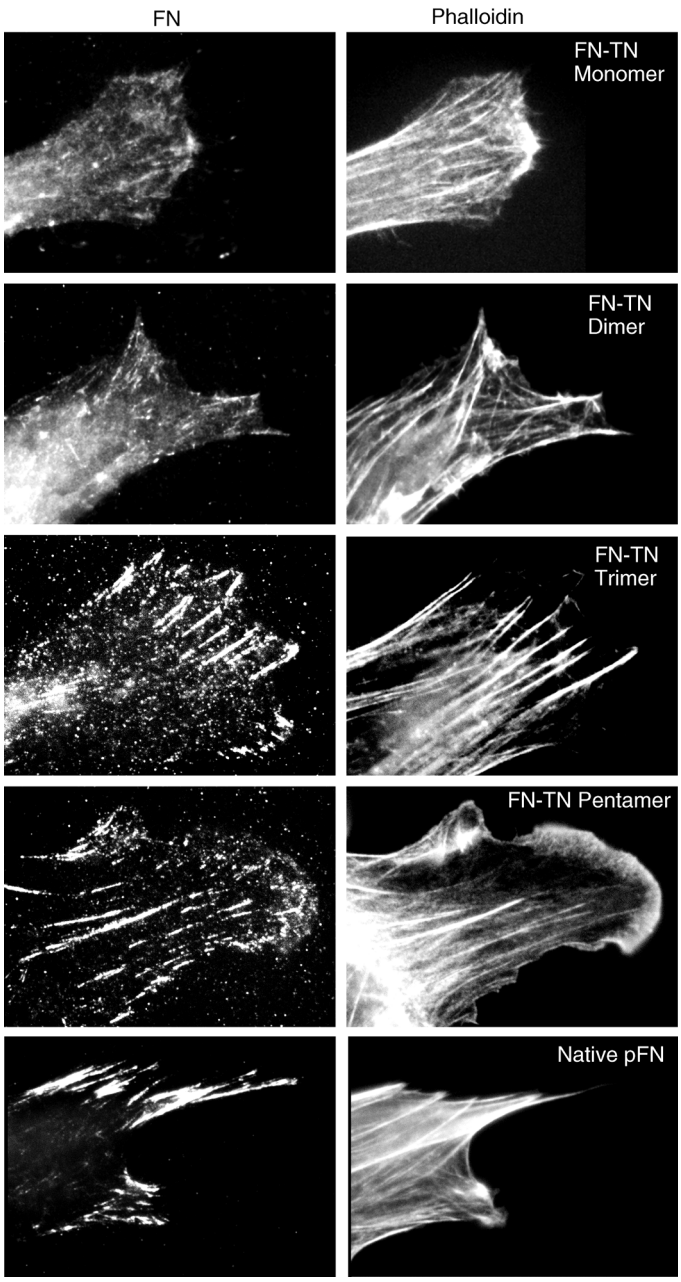

Fig. 6. Localization of FN oligomers over actin fibers. Cells were treated for 5 minutes with different FN-TN constructs and then fixed and labeled simultaneously with avidin to localize the FN-TN, and with phalloidin to localize actin polymers. The FN-TN streaks produced by the trimer and pentamer are always localized over actin fibers, but only a sub-set of the actin fibers is decorated. The streaks of plasma FN were shorter and more peripheral than those of FN-TN trimer and pentamer, and localized over shorter segments of actin fibers.

to integrins is rapidly reversible, and the engaged integrin does not show sustained binding to the cytoskeleton. Beads carrying the FN-FN tandem dimer, or the FN-TN dimer, frequently displayed a peculiar behavior: a low diffusion coefficient, suggesting binding to cytoskeletal elements, but no rearward movement. In contrast, beads coated with trimeric FN7-10 remained bound for longer than 10 seconds, and displayed a reproducible rearward movement. We had problems coating beads with the FN-TN pentamer, but the small number of bound beads behaved similarly to the trimer beads.

The collected observations of beads coated with different constructs are given in Table 1. These observations of bead tracking confirm that a monomeric FN7-10 produced a transient binding with free diffusion, while a single trimeric FN7-10 induced attachment of the integrin complex to the cytoskeleton, which is moving rearward.

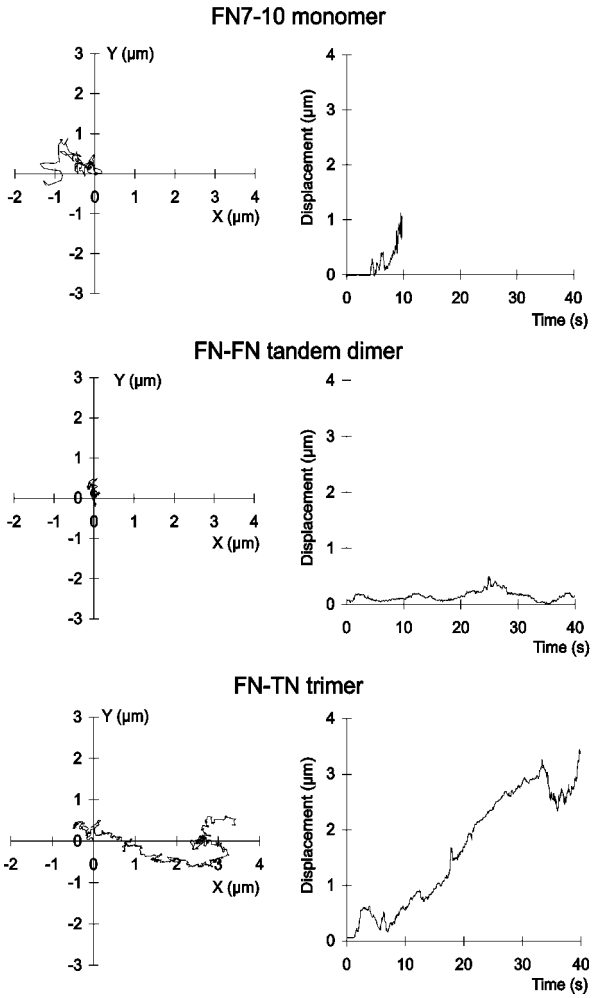

Fig. 7. Movement of latex beads coated with the different proteins. (Left traces) X versus Y plots of bead movement in the plane of the membrane. (Right traces) Displacement versus time of beads. At time zero, the beads were placed with the optical trap near the leading edge of the cell and maintained on the cell surface for 4 seconds. The laser was then stopped and the bead released. Unbound beads quickly drifted out of focus while bound beads remained on the cell surface.

Discussion

The cells used for binding studies were plated on laminin overnight, presumably forming focal contacts with α2β1 integrins, leaving the α5β1 integrins diffusely distributed on the upper cell surface (Fath et al., 1989) (Fig. 5). The functional unit in all our constructs was FN7-10, whose primary receptor is the integrin α5β1. We anticipate that the constructs with 2, 3 or 5 units of FN7-10 should be able to make clusters of 2, 3 or 5 integrins, although it is possible that the number of bound integrins is smaller than this maximum.

We considered the possibility that the trimer and pentamer might be aggregating, so that the active complex is actually larger than a trimer. Gradient sedimentation and high speed sedimentation demonstrated aggregation of trimer and pentamer at 2 mg/ml protein concentrations, but not at the 0.3 mg/ml used for the experiments. Finally, we note that the activity of the soluble complexes was confirmed in the bead translocation, where we believe only a single molecule is on the bound bead.

We tested the ability of FN7-10 monomer to compete with binding of the trimer, expecting the trimer to bind with much higher avidity than monomer. Martin et al. tested the ability of ICAM to block rhinovirus infection, and found that a bivalent IgA construct inhibited different viral activities at 40-200-fold lower concentrations than the monomer (Martin et al., 1993). Yet in our studies we found that 0.5 μM trimer could be competed by only an approximately fivefold excess of FN7-10 monomer. One difference is that the virus presented a rigid, multivalent target, whereas the integrin receptors on cells are diffusing in the plane of the membrane. When one arm of a trimer is released from the virus, its receptor on the virus remains in place facilitating rebinding. When one arm of a trimer is released from the cell surface, its integrin receptor is free to diffuse away. It can only rebind when an unbound integrin diffuses back into range. Thus the avidity may be much less for binding multivalent constructs to freely diffusible cell surface receptors than to a virus.

We had expected the dimeric constructs to produce most of the effects of the trimer and pentamer, as receptor dimerization is an established paradigm for activation (Heldin, 1995). It seems that a pair of integrins, like the monomer, may be too weak to form a stable attachment to the cytoskeleton, while a trimer, and even more a pentamer, provide sufficient contact sites to form a stable complex. Another possibility is that a dimer is the active species, but the formation of a dimeric complex of integrins is inefficient and requires three or more FN arms to get two efficiently bound to integrins.

Integrins localize to focal adhesions when activated by ligand occupancy or by exposing the β1 tail, and there is no requirement for clustering (Briesewitz et al., 1993; LaFlamme et al., 1992). The localization to actin fibers that we observed required clustering. This suggests that focal adhesions may present stronger binding sites for activated integrins than the actin fibers. We can conclude from the present studies that these actin fibers do have an affinity for activated integrins, but it generates a strong binding only when they are in clusters.

The existence of a rearward-moving cytoskeleton with integrin-binding capacity was suggested as the basis for the movement of beads coated with FN7-10 (Felsenfeld et al., 1996). These beads at first moved randomly on the cell surface, then began a linear, rearward movement. Attachment of the beads to these cytoskeletal tracks required clustering as well as integrin activation, since beads coated with a low concentration of FN7-10 showed only transient, diffusive movement. The clusters required for this attachment had to be small, since the beads were only 40 nm in diameter. Given the 8-12 nm size of the integrins, no more than five to ten FN7-10 molecules could be arranged on one side of the bead to form an integrin cluster. We believe that the soluble FN7-10 oligomers we have tested here are behaving like the beads. The soluble oligomers provide the important advantage that they can decorate completely the cytoskeletal tracks responsible for bead movement.

Two studies have investigated the effects of clustering integrins or their ligands. Hato et al. made a chimera of FK506-binding proteins with the integrin cytoplasmic tail, and used this to form clusters of integrins (Hato et al., 1998). These clusters failed to decorate an actin cytoskeleton. This may be

due to the absence of a cytoskeleton in these suspended cells, or may indicate that ligand binding is required in addition to clustering. Stupack et al. showed that adhesion of lymphoid cells to a multivalent fibrin matrix stimulated syk kinase, which in turn substantially enhanced the integrin affinity and adhesion (Stupack et al., 1999). It is becoming clear that integrin clustering, signalling and affinity modulation are complementary processes in adhesion.

This work was supported by NIH grants CA47056 (H.P.E.) and NS23345 (M.P.S.), and a grant from the Jonan Foundation to H.P.E.

References

Aukhil, I., Joshi, P., Yan, Y. and Erickson, H. P. (1993). Cell- and heparin-binding domains of the hexabrachion arm identified by tenascin expression proteins. *J. Biol. Chem.* **268**, 2542-2553.

Beck, K., Gambee, J. E., Bohan, C. A. and Bachinger, H. P. (1996). The C-terminal domain of cartilage matrix protein assembles into a triple-stranded α-helical coiled-coil structure. *J. Mol. Biol.* **256**, 909-923.

Briesewitz, R., Kern, A. and Marcantonio, E. E. (1993). Ligand-dependent and -independent integrin focal contact localization: the role of the alpha chain cytoplasmic domain. *Mol. Biol. Cell* **4**, 593-604.

Carrell, N. A., Fitzgerald, L. A., Steiner, B., Erickson, H. P. and Phillips, D. R. (1985). Structure of human platelet membrane glycoproteins IIb and IIIa as determined by electron microscopy. *J. Biol. Chem.* **260**, 1743-1749.

Choquet, D., Felsenfeld, D. P. and Sheetz, M. P. (1997). Extracellular matrix rigidity causes strengthening of integrin-cytoskeleton linkages. *Cell* **88**, 39-48.

Chung, C. Y., Zardi, L. and Erickson, H. P. (1995). Binding of tenascin-C to soluble fibronectin and matrix fibrils. *J. Biol. Chem.* **270**, 29012-29017.

Efimov, V. P., Engel, J. and Malashkevich, V. N. (1996). Crystallization and preliminary crystallographic study of the pentamerizing domain from cartilage oligomeric matrix protein: A five-stranded α-helical bundle. *Proteins* **24**, 259-262.

Fath, K. R., Edgell, C.-J. S. and Burridge, K. (1989). The distribution of distinct integrins in focal contacts is determined by the substratum composition. *J. Cell Sci.* **92**, 67-75.

Felsenfeld, D. P., Choquet, D. and Sheetz, M. P. (1996). Ligand binding regulates the directed movement of beta1 integrins on fibroblasts. *Nature* **383**, 438-440.

Fowler, W. E. and Erickson, H. P. (1979). Trinodular structure of fibrinogen. Confirmation by both shadowing and negative stain electron microscopy. *J. Mol. Biol.* **134**, 241-249.

Gelles, J., Schnapp, B. J. and Sheetz, M. P. (1988). Tracking kinesin-driven movements with nanometre-scale precision. *Nature* **331**, 450-453.

Hato, T., Pampori, N. and Shattil, S. J. (1998). Complementary roles for receptor clustering and conformational change in the adhesive and signaling functions of integrin alpha(IIb)beta(3). *J. Cell Biol.* **141**, 1685-1695.

Heldin, C. H. (1995). Dimerization of cell surface receptors in signal transduction. *Cell* **80**, 213-223.

Kuo, S. C. and Sheetz, M. P. (1993). Force of single kinesin molecules measured with optical tweezers. *Science* **260**, 232-234.

LaFlamme, S. E., Akiyama, S. K. and Yamada, K. M. (1992). Regulation of fibronectin receptor distribution. *J. Cell Biol.* **117**, 437-447.

Leahy, D. J., Aukhil, I. and Erickson, H. P. (1996). 2.0 Å crystal structure of a four-domain segment of human fibronectin encompassing the RGD loop and synergy region. *Cell* **84**, 155-164.

Malashkevich, V. N., Kammerer, R. A., Efimov, V. P., Schulthess, T. and Engel, J. (1996). The crystal structure of a five-stranded coiled-coil in COMP: a prototype ion channel? *Science* **274**, 761-765.

Martin, S., Casanovas, J. M., Staunton, D. E. and Springer, T. A. (1993). Efficient neutralization and disruption of rhinovirus by chimeric ICAM-1/immunoglobulin molecules. *J. Virol.* **67**, 3561-3568.

Melby, T. E., Ciampaglio, C. N., Briscoe, G. and Erickson, H. P. (1998). The symmetrical structure of structural maintenance of chromosomes (SMC) and MukB proteins: long, antiparallel coiled coils, folded at a flexible hinge. *J. Cell Biol.* **142**, 1595-1604.

Miyamoto, S., Akiyama, S. K. and Yamada, K. M. (1995a). Synergistic roles for receptor occupancy and aggregation in integrin transmembrane function. *Science* **267**, 883-885.

Miyamoto, S., Teramoto, H., Coso, O. A., Gutkind, J. S., Burbelo, P. D., Akiyama, S. K. and Yamada, K. M. (1995b). Integrin function: Molecular hierarchies of cytoskeletal and signaling molecules. *J. Cell Biol.* **131**, 791-805.

Nermut, M. V., Green, N. M., Eason, P., Yamada, S. S. and Yamada, K. M. (1988). Electron microscopy and structural model of human fibronectin receptor. *EMBO J.* **7**, 4093-4099.

Qian, H., Sheetz, M. P. and Elson, E. L. (1991). Single particle tracking. Analysis of diffusion and flow in two-dimensional systems. *Biophys. J.* **60**, 910-921.

Sayle, R. A. and Milner-White, E. J. (1995). RASMOL: biomolecular graphics for all. *Trends Biochem. Sci.* **20**, 374.

Schmidt, C. E., Horwitz, A. F., Lauffenburger, D. A. and Sheetz, M. P. (1993). Integrin-cytoskeletal interactions in migrating fibroblasts are dynamic, asymmetric, and regulated. *J. Cell Biol.* **123**, 977-991.

Studier, F. W., Rosenberg, A. H., Dunn, J. J. and Dubendorff, J. W. (1990). Use of T7 RNA polymerase to direct expression of cloned genes. *Methods Enzymol.* **185**, 60-89.

Stupack, D. G., Li, E. G., Silletti, S. A., Kehler, J. A., Geahien, R. L., Hahn, K., Nemerow, G. R. and Cheresh, D. A. (1999). Matrix valency regulates integrin-mediated lymphoid adhesion via Syk kinase. *J. Cell Biol.* **144**, 777-787.

Tomschy, A., Fauser, C., Landwehr, R. and Engel, J. (1996). Homophilic adhesion of E-cadherin occurs by a co-operative two-step interaction of N-terminal domains. *EMBO J.* **15**, 3507-3514.

Tripet, B., Vale, R. D. and Hodges, R. S. (1997). Demonstration of coiled-coil interactions within the kinesin neck region using synthetic peptides. Implications for motor activity. *J. Biol. Chem.* **272**, 8946-8956.